Mansoura Engineering Journal

Volume 31 | Issue 4 Article 11

10-10-2021

Study of Parameters Affecting Thermal Drying Process.

Mohamed Wasel
Professor of Mechanical Power Engineering Department., Faculty of Engineering., El-Mansoura University., Mansoura., Egypt.

Hesham Mostafa
Mechanical Engineering Department., Higher Technological Institute., Tenth of Ramadan City., Egypt., drheshammostafa@yahoo.com

Gamal Sultan
Associate Professor., Mechanical Power Engineering Department., Faculty of Engineering., El-Mansoura University., Mansoura., Egypt., gisultan@mans.edu.eg

A. Abd El-Badie
Research Student

Recommended Citation

Wasel, Mohamed; Mostafa, Hesham; Sultan, Gamal; and Abd El-Badie, A. (2021) "Study of Parameters Affecting Thermal Drying Process.," *Mansoura Engineering Journal*: Vol. 31 : Iss. 4 , Article 11.
Available at: https://doi.org/10.21608/bfemu.2021.198876

STUDY OF PARAMETERS AFFECTING THERMAL DRYING PROCESS

دراسة عوامل مؤثرة على عملية التجفيف الحرارى

M. G. Wasel*, Hesham M. Mostafa, Gamal. I. Sultan* and A. Abd El-Badie*****

* Faculty of Engineering, Mansoura University, Mansoura, Egypt.

** Higher Technological Institute, Tenth of Ramadan City, Egypt.

*** Research student

Email: DrHeshamMostafa@yahoo.com

Email: gisultan@mans.edu.eg

خلاصة البحث:

فـى هـذا البحث تمت دراسة عوامل مؤثرة على عملية التجفيف عمليا وما يصحب ذلك من إنتقال للحرارة وإنتقال للكتلة مابين الوسط المسامى المبتل المراد تجفيفه والهواء الذى يمر خلال ذلك الوسط. لإتمام هذه الدراسة تم تصميم وتنفيذ دائرة إختبار معملية تـتكون من مجرى أنبوبى دائرى رأسى موجود بداخله الوسط المسامى المبتل وهو عبارة عن كرات من الطوب المسامى المشبع بالمـاء. تحـدث عمليـة التجفيف نتيجة لدفع الهواء الساخن جبريا رأسيا لأعلى ليمر خلال الوسط المسامى المبتل فيحدث تبخير للـرطوبة الموجـودة فى ذلك الوسط بفعل إنتقال الحرارة وإنتقال الكتلة الآنيين. ظروف التشغيل المختبرة هى معدل تدفق الهواء ودرجـة حرارته وطول الوسط المسامى ومسامية كرات الطوب. وتم حساب معامل إنتقال الحرارة المتوسط ومعامل إنتقال الكتلة المتوسط لسريان الهواء الساخن خلال الوسط المسامى المبتل.

وقد أظهرت النتائج أن عملية التجفيف تزيد مع زيادة معدل تدفق الهواء ودرجة حرارته ومسامية كرات الطوب وتقل مع زيادة طـول الوسـط المسامى. وأيضا معامل إنتقال الحرارة المتوسط ومعامل إنتقال الكتلة المتوسط لسريان الهواء الساخن خلال الوسط المسـامى المبتل يزيد مع زيادة معدل تدفق الهواء ودرجة حرارته ومسامية كرات الطوب وتقل مع زيادة طول الوسط المسامى. وتمت مقارنة النتائج مع نتائج معملية سابقة حيث أعطت نفس الإتجاه.

Abstract

Parameters affecting drying process has been studied experimentally as it associated with heat and mass transfer between porous bed to be dried and air which flows through the porous bed. To perform this study, a test rig is designed and constructed as it consists of vertical circular duct packed with wet porous bed which is made from clay balls of 20 mm in diameter. Drying process occurs as a result of forcing hot air vertically to pass through the wet porous bed, evaporation of moisture is existed in the bed due to the simultaneous heat and mass transfer. The studied operating parameters are inlet air temperature, inlet air mass flux, porous bed depth and porosity of balls. The average heat and mass transfer coefficients are estimated for flow of hot air through the wet porous bed.

The results indicated that, the drying rate is directly proportional to inlet air temperature, mass flux of air, dimensionless bed depth and ball porosity. So, Drying process can be achieved in lower time as increasing both air mass flux and or inlet air temperature and decreasing bed depth. Also, heat transfer coefficient and mass transfer coefficient increase with increasing inlet air temperature, inlet air mass flux, and ball porosity, but they decrease with increasing bed depth. Comparison between the obtained experimental results and the previous work gave the same trend.

Key words: Heat and mass Transfer, drying, and wet porous bed.

1. INTRODUCTION

Drying is widely used in thermal energy applications. Industrial applications for drying include the production of paper, textiles, food industries and agricultural products, chemical products, building and construction materials, and many others. Thermal drying is the removal of a liquid from a material through thermal treatment. Thermal drying process requires a lot of energy for evaporating the moisture. The traditionally drying medium is the hot air.

Accepted October 18, 2006

The main controlling parameters for the drying processes are: the temperature and pressure of the drying medium, the slip velocity and the humidity if air used as drying medium.

Theoretical and experimental validation for drying characteristics of banana was studied by Karim and Hawlader (2005). The model includes the influence of both material and equipment, is capable of predicting dynamic behavior of the dryer. The material model is capable of predicting the instantaneous temperature and moisture distribution inside the material. Also, the study was conducted to examine the effect of different operating variables on drying potential and drying time.

Mathematical modeling of high quality pasta drying is investigated by Migliori et al. (2005). The mass and heat exchange between pasta samples and air was modeled according to the classic transport approach applied to hollow cylindrical shape pasta.

Mathematical simulation of convection food batch drying with assumptions of plug flow and complete mixing of air was studied by Herman-Lara et al. (2005). They took into account heat and mass transfer to air, product and interface along with water thermodynamic equilibrium. Also the study indicated that air outlet temperature is a way of showing deviations from air plug flow behavior.

Babalis and Belessiotis (2004) studied numerically and experimentally the influence of drying air characteristic on the drying performance of figs. The influence of drying air temperature in the range of 55- 85 C° and of the air velocity in the range from 0.5 to 3 m/s, for figs was studied. A range of 1-2 m/s drying air velocity has to be preferably established inside an industrial dryer for agriculture products, giving the best cost/efficiency performance for the drying of figs.

Sander et al. (2003) reported that, the drying air temperature, and initial material moisture content of clay slab strongly influence the drying kinetics and transport properties. Effective diffusion coefficient, heat and mass transfer coefficients, and thermal conductivity, are the main transport properties of thin clay plate (drying temperature and initial moisture content).

Peters et al. (2002) studied theoretically and experimentally the drying of a packed bed. Within the experiments both single particle and packed bed measurements for the drying of wood were carried out. The results showed that, a particle resolved approach is better suited than a continuum mechanic approach to describe packed bed processes.

Numerical simulation of grain drying in vertical bed has been carried out by Mhimid et al. (2000). Two mathematical models of heat and mass transfer are examined and adapted from the general porous medium theory of Patankar (1980). These models are local temperature equilibrium model and not local temperature equilibrium model. The heat and mass transfer model which was used took into considerations drying by forced convection and conduction heating at the wall and higher porosity near the wall. The results reveal that complementary drying by wall heating is not efficient as convective heating.

Wang and Chen (1999) studied numerically the heat and mass transfer in fixed-bed drying. The temperature, moisture content and pressure distributions in the particle were considered. Their results showed that non-uniformity existed not only for temperature and relative humidity of gas in the fixed-bed, but also for the temperature, moisture content and pressure in the material. Also, their results showed that a drying front existed in the fixed bed and moved forward linearly with drying time.

Simal et al. (1994) studied theoretically and experimentally the heat and mass transfer during hot air drying of potato cubes. The moving boundary problem was solved by an explicit finite difference method using experimental data of an experiment carried out at 90°C.

Arnaud and Fohr (1988) studied numerically, slow drying process for airflow

though wet porous medium, which simulate thick layers of granular products. The obtained model leads to an examination of the validity of preceding simplified models and the more general solution of continuous drying.

Renken and Poulikakos (1987) studied experimentally and theoretically forced convection heat transfer in a packed bed of spheres. A parallel plate channel configuration with walls maintained at constant temperature was employed. Their results document the dependence of the temperature field as well as the heat flux from the wall on the problem parameters in the thermally developing region. The Nusselt number measurements showed a significant increase in the local heat transfer at the channel wall relative to that in classical fluids.

Dutta et al. (1987) studied theoretically and experimentally the drying behavior of spherical grains. The drying characteristic of the grain are similar to those of other grains belonging to the same category in the falling rate period.

In this work, the study is done to investigate the effect of the affecting parameters on the drying process such as air flow rate, air inlet temperatures, bed depth and ball porosity.

2. EXPERIMENTAL APPRATUS

The experimental apparatus is designed and constructed to study parameters affecting the drying process for wet porous medium. Figure (1-a) shows a schematic diagram for the experimental apparatus. It consists mainly of vertical circular duct which contained air blower (1) electric heater (3), entrance section (5) and the test section (8). At the inlet section before the air blower, a throttle plate gate (2) is fixed and used to control the airflow rate through the tested bed and to obtain the desired value of air mean velocity. The air blower draws air from the surroundings and passes it over two electric heaters (3), each one having 1.5 kW rated power. The input power supplied to the electric heaters is controlled by using variac (12), to select the required input power accurately. Air is heated to the desired condition, and then it flows through the wet porous bed inside the vertical duct. A flexible connection (4) between the air blower and the vertical duct is used to damp any vibration associated with the airflow. To insure that the fully developed condition is reached for the flowing of hot air at inlet to the test section, air is passed through the entrance section (1m long). The main details of the test section are illustrated in Fig. (1.b).

The test section is of 105 mm in diameter and 210 mm in length. This length can be varied along the experiments up to 52.5 mm. The tested porous bed (15) is packed with a uniform 20 mm in diameter wet porous clay balls. The total number of balls was 198 and the bed porosity "volume of air between balls to the total volume of bed" is about 0.54. Two kinds of balls are tested in this work with internal ball porosity "void volume in each ball to the total volume of each ball" of 0.6 and 0.7, respectively. Two stainless steel screens (13) are placed at both ends of the tested bed to hold the balls in its place. Both portions of the test section are to be removable so that the test section is packed easily into its place. Therefore the weight of the tested bed can be measured easily before and after each experiment. To minimize heat loss from the test section, a 50-mm thickness of glass wool (14) is used to insulate the outer surfaces of the test section and the remaining duct.

3. EXPERIMENTAL DATA

The experimental apparatus is provided with sensors to measure temperatures, relative humidity, air velocity and mass of evaporated water through each experiment. For each experiment, the experimental apparatus is allowed to operate until steady state condition is reached when the fluctuation in outlet air temperature from electric heaters is about ±0.1 °C. Once the system reached the desired steady state condition, the test section, which contains the wet porous bed is placed in its location. At this moment the required measurements

are taken. All measurements are collected and recorded for further analysis.

Relative humidity (RH) is measured at upstream and downstream of the test section by using a hygrometer sensor (type Testo 605-H1), with a resolution of 0.1% and accuracy of ±3%. Also, dry bulb and dew point temperatures are measured at upstream and downstream of the test section by using the same sensor with a resolution of 0.1 °C and accuracy of ±0.5 °C.

Air velocity at upstream of the test section, is measured by using hot wire anemometer sensor (type Testo 605-V1), with a resolution of 0.01 m/s and accuracy of ±0.05 m/s. Then the average value of air velocity can be calculated from five measurements at different radii. The weight of the tested bed is measured before and after each experiment by using a digital mass balance (11) with a sensitivity of ±0.1 g. Therefore, the mass of the evaporated water from the tested bed can be calculated. The input electric power supplied to the electric heaters is measured by measuring the input voltage and current. The minimum readable values for voltage and current are ±0.1 V and ±0.01 A, respectively.

In order to obtain a measure of the reliability of the experimental data an uncertainty analysis was performed for the principle parameters of interest. The root-mean-square random error propagation analysis is carried out in the standard fashion using uncertainties of the basic independent variables (experimentally measured). These variables are bed dimensions, temperatures, relative humidity, air velocity, and mass of evaporated water, which used to calculate the uncertainty in Nusselt number and Sherwood number. The largest calculated uncertainties in the current investigation are less than 8.6% for Nusselt number and 11.5% for Sherwood number.

4. DATA REDUCTION

To perform the required analysis for the obtained experimental data, the air and water vapor in the duct is treated as ideal gases.

Air flow rate inlet to the duct can be calculated as;

$$\dot{m}_{air} = \rho_{air} u_{av} A_c \qquad (1)$$

where A_c , ρ_{air} and u_{av} are cross section area of duct ($A_c = \frac{\pi}{4} d^2$), air density at inlet to the test section and average velocity of air at inlet to the test section, respectively. The average velocity at inlet to the test section is obtained by integration of local velocity across the cross-sectional area of duct.

The mass flow rate of water vapor which evaporated from the wet porous bed can be calculated as;

$$\dot{m}_{ev} = \dot{m}_{air}\left(\bar{\omega}_{out} - \bar{\omega}_{in}\right) \qquad (2)$$

Where $\bar{\omega}_{in}$ and $\bar{\omega}_{out}$ are the humidity ratios of air at inlet and outlet to the test section, respectively (moist air properties are known at inlet and outlet of the test section).

The drying process caused by hot air flows through the wet porous bed, i.e. evaporation of water from surface of balls to air flows through the bed due to concentration difference. The convective heat transfer from airflow to ball surface cause a decrease in the outlet air temperature. Also part of heat consumed by water vapor itself (which found at saturation temperature) to reach the outlet air temperature. The convective heat transfer (Q_{con}) and evaporative heat transfer (Q_{ev}) are calculated as;

$$Q_{con} = \dot{m}_{air} Cp_{air}\left(T_{db,in} - T_{db,out}\right) \qquad (3)$$

$$Q_{ev} = \dot{m}_{ev}\left[h_{fg} - Cp_v\left(T_{db,out} - T_{sat}\right)\right] \qquad (4)$$

Where $\dot{m}_{ev}$, h_{fg}, $\dot{m}_{air}$, Cp_{air}, Cp_v, $T_{db,in}$, $T_{db,out}$, T_{sat} are the evaporation rate, the latent heat of vaporization, the airflow rate, the specific heat at constant pressure for air, the specific heat at constant pressure for water vapor, the inlet air dry bulb temperature, the outlet air dry bulb temperature, and water vapor saturation temperature, respectively.

The density of the superheated water vapor in the inlet air to the test section at the dry bulb temperature is determined from;

$$\rho_{v,in} = \frac{P_v}{R_v T_{in,db}} \quad (5)$$

Where R_v and $T_{in,db}$ are gas constant for water vapor and dry bulb temperature for inlet air to the test section respectively.
The water vapor pressure P_v in the inlet air to the test section was calculated from;

$$P_v = \frac{\omega_{in} P_{atm}}{0.622 + \omega_{in}} \quad (6)$$

where P_{atm} is the atmospheric pressure.
At the air-bed surface interface, the air is saturated with water vapor. The density of the saturated water vapor at initial value of bed surface temperature is obtained from;

$$\rho_{v,bed,i} = \frac{P_{sat}}{R_v T_{bed,i}} \quad (7)$$

Where P_{sat} is the saturated pressure for water vapor corresponding to the initial value of bed surface temperature at the begging of the experiment and $T_{bed,i}$ is the water vapor temperature which equal to the bed temperature at inlet to the experiment.

The instantaneous values of convective heat transfer coefficient (h_{con}), evaporative heat transfer coefficient (h_{ev}) and mass transfer coefficient (h_m) can be defined as;

$$h_{con} = \frac{Q_{con}}{A_s(T_{db,in} - T_{bed,i})} \quad (8)$$

$$h_{ev} = \frac{Q_{ev}}{A_s(T_{db,in} - T_{bed,i})} \quad (9)$$

$$h_m = \frac{m_{ev}}{A_s(\rho_{v,bed,i} - \rho_{v,in})} \quad (10)$$

Where A_s is surface area of the bed which is defined as;

$$A_s = \frac{3V_{solid}}{r} \quad (11)$$

Where r is the radius of ball and V_{solid} is the volume of porous solid material which can be defined as;

$$V_{solid} = \frac{\pi}{4} d^2 L(1 - \epsilon_{bed}) \quad (12)$$

Where d, L and ϵ_{bed} are the bed diameter, bed depth and bed porosity, respectively.

Accordingly, local values of Nusselt number (based on convection only and evaporation only) and Sherwood number are calculated as;

$$Nu_{con} = \frac{h_{con} L}{k} \quad \& \quad Nu_{ev} = \frac{h_{ev} L}{k} \quad (13)$$

$$Sh = \frac{h_m L}{D} \quad (14)$$

Where k and D are thermal conductivity of air, and diffusion coefficient of water vapor in air at average dry bulb temperature, respectively.
Average Nusselt and Sherwood numbers are defined as;

$$\overline{Nu_{con}} = \frac{1}{\tau}\int_0^t Nu_{con}\, dt \quad (15)$$

$$\overline{Nu_{ev}} = \frac{1}{\tau}\int_0^t Nu_{ev}\, dt \quad (16)$$

$$\overline{Sh} = \frac{1}{\tau}\int_0^t Sh\, dt \quad (17)$$

5. Results and Discussion

The effect of temperature and mass flux of inlet hot air, bed depth and ball porosity on the drying process are analyzed experimentally. Suitable analyses for the experimental measurements lead to obtain the heat and mass transfer coefficients. Consequently, Nusselt and Sherwood numbers are obtained.

Figure (2) shows the variation of the direct measured values of the outlet air temperature with respect to time, for certain value of mass flux of air (G=1 kg/m^2.s) through the first bed (ϵ_b = 0.6) at different inlet air temperatures. It is clear from the figure that, outlet air temperature increases with time and reaches an asymptotic value after a certain time. This value for the outlet air temperature is less than the inlet air temperature by a few degrees in each case. As expected, increasing inlet air temperature led to increase the outlet air temperature in a short time.

The effect of inlet hot air temperature on outlet humidity ratio for air is presented in Fig. (3), for certain air mass flux through the first bed. It is clear that the outlet air humidity ratio increases suddenly from the initial value to the maximum value in the first few minutes for each experiment. At the beginning of the experiment, the outlet humidity ratio increases with increasing inlet air temperature. For higher values of inlet air temperatures, the humidity ratio decreases with time dramatically until it reaches a certain value after which there is a very small decrease in outlet humidity ratio. Then, the humidity ratio attains a constant value which approximately equals to the initial value. Therefore, the drying time (which is defined as the required time for complete drying) is obtained. Also it is clear that, the drying time decreases with increasing inlet air temperatures.

The evaporation rate for water vapor from porous bed to the flowing air (m'_{ev}) is calculated from equation (2) and plotted against time of the experiment for different inlet air temperatures, as shown in Fig. (4.a). It is observed from the figure that, at the beginning of the experiment the evaporation rate possess higher values with increasing inlet air temperatures. Also, it is noticed that, for higher values of inlet air temperatures the evaporation rate from the porous bed decrease dramatically with time. But, for lower values of inlet air temperatures, at the beginning of the experiment, the decrease in evaporation rate are small, which equivalent to constant drying period. Then, with increasing the experiment time the falling period was obtained. Figure (4.b) shows the variation of the evaporation rate for water vapor against time for different values of mass fluxes of air at an inlet air temperature of $T_{air,in}$ = 40 °C. It is noticed that, at the beginning of the experiment the evaporation rate increases as air mass flux increases.

The difference between weight of the wet porous bed and the dry porous bed is known as the initial amount of water exists in the bed at the beginning of each experiment. From the experimental data for temperatures and humidity ratio the amount of water evaporated at any time along the experiment is obtained. Therefore, moisture content is defined as the ratio between the remaining amount of water in the bed (the difference between the initial amount of water exists in the bed at the beginning of each experiment and the amount of water evaporated at a certain time) to the initial amount of water exists in the bed at the beginning of each experiment. The percentage of moisture content versus time for different inlet air temperatures is illustrated in Fig. (5). The drying time is known as the required time to evaporate the initial water content in the bed. This time can be easily obtained from Fig. (5) at zero moisture content and it is clear that, the drying process can be achieved in a lower time as inlet air temperature increases for a certain value of inlet air mass flux. Also, increasing the air inlet temperature from 30°C to 60 °C led to decrease the drying time from 420 min to 180 min, respectively.

Figure (6) shows the effect of inlet air mass flux on the drying time for different values of inlet air temperatures. It is observed that, drying time decreases as air mass flux and or inlet air temperature increases. Therefore complete drying can be achieved in lower time as air mass flux and inlet air temperature increase. The increase of inlet air mass flux from 1 to 4 kg/s/m^2 led to a decrease of the drying time from 180 min to 32 min at 60 °C air inlet temperature. But this decrease in drying time is from 420 to 100 min at air inlet temperature of 30 °C.

The average values for convective and evaporative heat transfer coefficients are calculated and plotted against air mass flux at different inlet air temperatures, as shown in Fig. (7). As it is expected the average heat transfer coefficients increase with increasing air mass flux for a certain value of inlet air temperature. Also, increasing inlet air temperature causes an increase in the convective and evaporative heat transfer rates.

In turn the average values for Nusselt number based on convection only and evaporation only are plotted in Fig.(8) against inlet air mass flux. As it is expected, Nusselt number behaves the same trend as heat transfer coefficient.

Sherwood number (Sh) is plotted against air mass flux at different inlet air temperatures, as shown in Fig. (9). It is observed that Sherwood number increases as air mass flux and inlet air temperature increase. This increase in Sh with the air mass flux is expected for the same inlet air temperature. But, for the same air mass flux, increasing inlet air temperature causes a decrease in water vapor concentration at the ball surface and this leads to an increase in Sh. The maximum enhancement in the average Sherwood number is about 340% as inlet air mass flux increases from 1 to 4 $kg/m^2.s$ at 60°C inlet air temperature, but this enhancement is 370% at 30°C air inlet temperature. Also, increasing the air inlet temperature from 30°C to 60 °C led to an increase in the average Sherwood number by about 300% at inlet air mass flux of 4 $kg/m^2.s$ and 200% when the inlet air mass flux is 1 $kg/m^2.s$.

Bed depth can be reduced from the initial value up to a smaller value to study the effect of bed depth on the drying process. Figure (10) shows the effect of bed depth on the average values of mass transfer coefficient, convective and evaporative heat transfer coefficients of air mass flux of 1 $kg/m^2.s$ and inlet air temperature of 30°C. It is clear that as bed depth increases the average values of mass transfer, convective and evaporative heat transfer coefficients are decreased. So, the drying rate is decreased.

The effect of ball porosity on the evaporation rate of water vapor is plotted for air mass flux, G=1 $kg/m^2.s$ and inlet air temperature, $T_{air,in}$= 40 °C, as shown in Fig. (11). Generally, the evaporation rate increases as ball porosity increases due to the increase in the void inside the balls and in turn the increase in the amount of initial water content.

The present experimental moisture content is compared with the previous experimental work, as shown in Fig. (12). The previous theoretical and experimental work; for Sander et al. (2003), was done for heat and mass transfer models in convection drying of clay slabs. This slabs put in circular cylindrical duct and hot air passes through it with velocity 0.43 m/s. The obtained experimental results and the previous work gave the same trend.

6. Conclusions

Simultaneous heat and mass transfer for drying process of air flows through a wet porous bed is experimentally studied. Drying process can be achieved in lower time as mass flux of air increases and or inlet air temperature increases. The evaporation rate is increased as the ball porosity increases due to the increase in the amount of initial water content. The heat transfer coefficient and mass transfer coefficient (or in turn Nusselt and Sherwood number) are increased with increasing inlet air temperature, inlet air mass flux, and ball porosity; but decreasing with the increase of bed depth. Comparison between the obtained experimental results and the previous work gave the same trend.

Nomenclature

A : Area, m^2
d : Bed diameter ,m
D : Diffusion coefficient, m^2/s
G : Mass flux, $kg/m^2.s$
h : Heat transfer coefficient, $W/(m^2.°C)$
h_m : Mass transfer coefficient, m/s
k : Thermal conductivity, W/(m. °C)
i : Enthalpy for air, J/kg
L : Bed length, m
m'_{air} : Airflow rate, kg/s
m'_{ev} : Evaporation rate, kg/s
Nu : Nusselt number (Nu=hL/k), -
P : Pressure, Pa
P_{atm} : Atmospheric pressure, atm
Q : Rate of heat transfer, W
r : Ball radius, m
R : Gas constant, $Pa.m^3/(kg.K)$
Sh : Sherwood number ($Sh=h_m L/D$), -

T : Temperature, °C
t : Time, s
u : Air velocity, m/s
V : Volume, m^3

Greek symbols

ε : porosity, -
ρ : Density, kg/m^3
ω : Humidity ratio, kg_v/kg_{air}
τ : Drying time, s

Subscripts

air	Air	eff	Effective
atm	atmospheric	ev	Evaporated
av	average	i	Initial
b	Ball	in	Inlet
bed	porous bed	m	Mass
c	cross section	out	Out
con	convection	sat	Saturation
d	dry	v	Water vapor
db	dry bulb	s	Surface

REFERENCES

[1] **Karim, M. D. and Hawlader, M. N. A.,** 2005 "Drying characteristics of banana theoretical modeling and experimental validation" Journal of food Engineering Vol.70, pp.35- 45.

[2] **Migliori, M., Gabriele, D., Cindio, B. D. and Pollini, C. M.,** 2005 " Modelling of high quality pasta drying mathematical model and validation " Journal of food Engineering Vol.69,pp.387- 397.

[3] Herman-Lara, E., Salgado-Cervantes, M. A. and Garc'a-Alvarado, M. A., 2005 "Mathematical simulation of convection food batch drying with assumptions of plug flow and complete mixing of air" Journal of food Engineering Vol. 68, pp. 321- 327.

[4] **Babalis, S. J. and Bellessiotis, V. G.,** 2004 "Influence of the drying condition on the drying constants and moisture diffusivity during the thin-layer drying of figs" 2004, Journal of food Engineering Vol.65, pp. 449- 458.

[5] **Sander, A., Skansi, D. and Bolf, N.,** 2003 " Heat and mass transfer models in convection drying of clay slabs " Ceramics international J., Vol. 29, pp. 641- 653.

[6] **Peters, B., Schroder, E., Bruch, C. and Nussbaumer, T.,** 2002 "Measurements and particle resolved modeling of heat-up and drying of a packed bed" Int. J. of Biomass and Bio-energy, Vol. 23, pp. 291-306.

[7] **Mhimid, A., Ben Nasrallah, S. and Fohr, J. P.,** 2000 "Heat and mass transfer during drying of granular products-simulation with convective and conductive boundary conditions" Int. J. Heat and Mass Transfer, Vol. 43, pp. 2779-2791.

[8] **Wang, Z. H. and Chen, G.,** 1999 "Heat and mass transfer in fixed-bed drying" Chemical Engineering Science, Vol. 54, pp. 4233-4243.

[9] **Simal, S., Rossell, C., Berna, A. and Mulet, A.,** 1994 "Heat and mass transfer model for potato drying" Int. J. Chemical Engineering Science, Vol. 49, No. 22, pp. 3739-3744.

[10] **Arnaud, G. and Fohr, J. P., 1988** "Slow drying simulation in thick layers of granular products" Int. J. Heat and Mass Transfer, Vol. 31, No.12, pp. 2517-2526.

[11] **Renken, K. J. and Poulikakos, D.,** 1987 "Experiment and analysis of forced convective heat transport in a packed bed of spheres" Int. J. Heat and Mass Transfer, Vol. 30, No. 7, pp. 1399-1408.

[12] **Dutta, S. K., Nema, V. K. and Bhardwaj, R. K.,** 1987 "Drying behavior of spherical grains" Int. J. Heat and Mass Transfer, Vol. 30, No. 4, pp. 855-860.

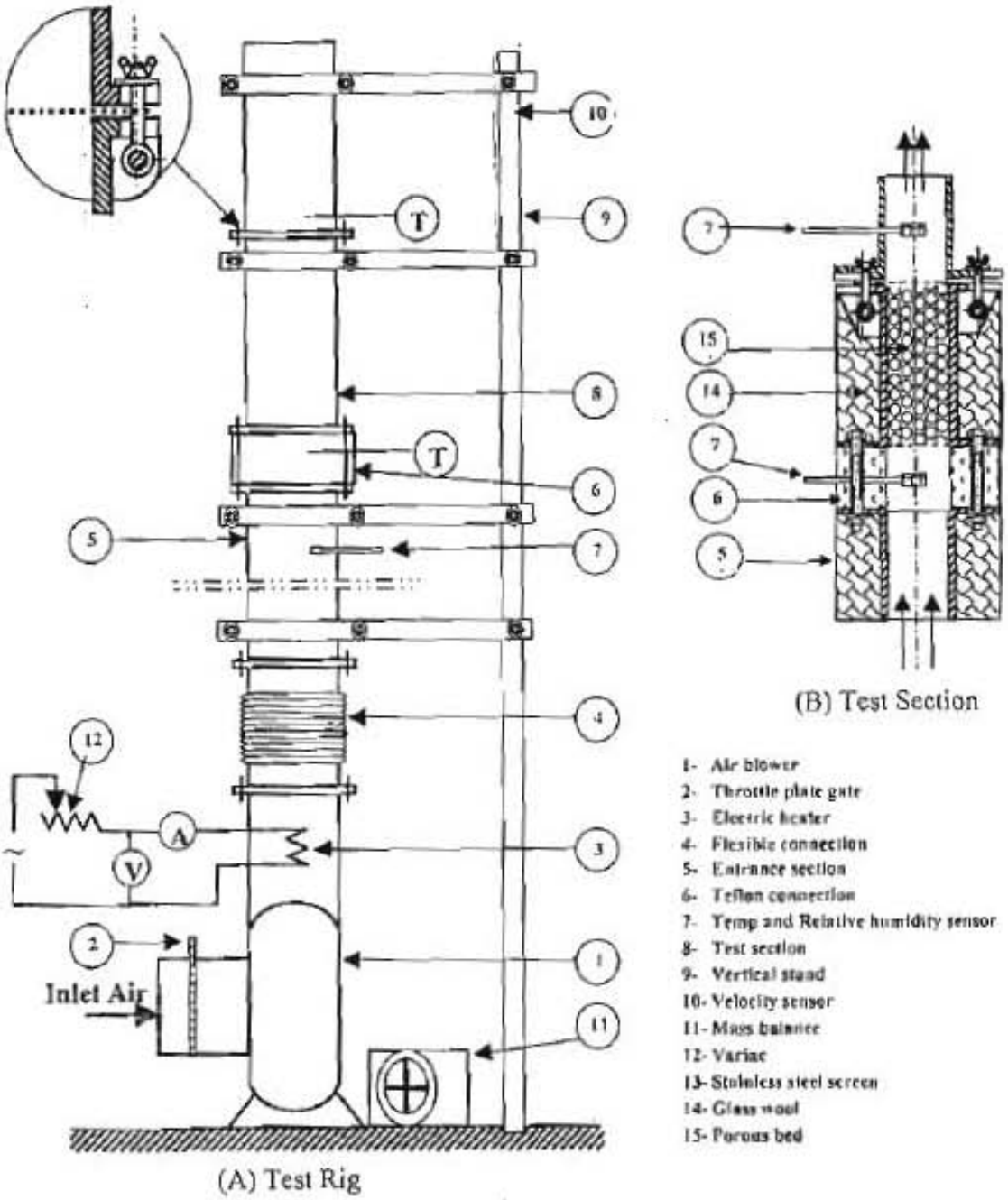

Fig. (1) Schematic diagram for the experimental apparatus and test section.

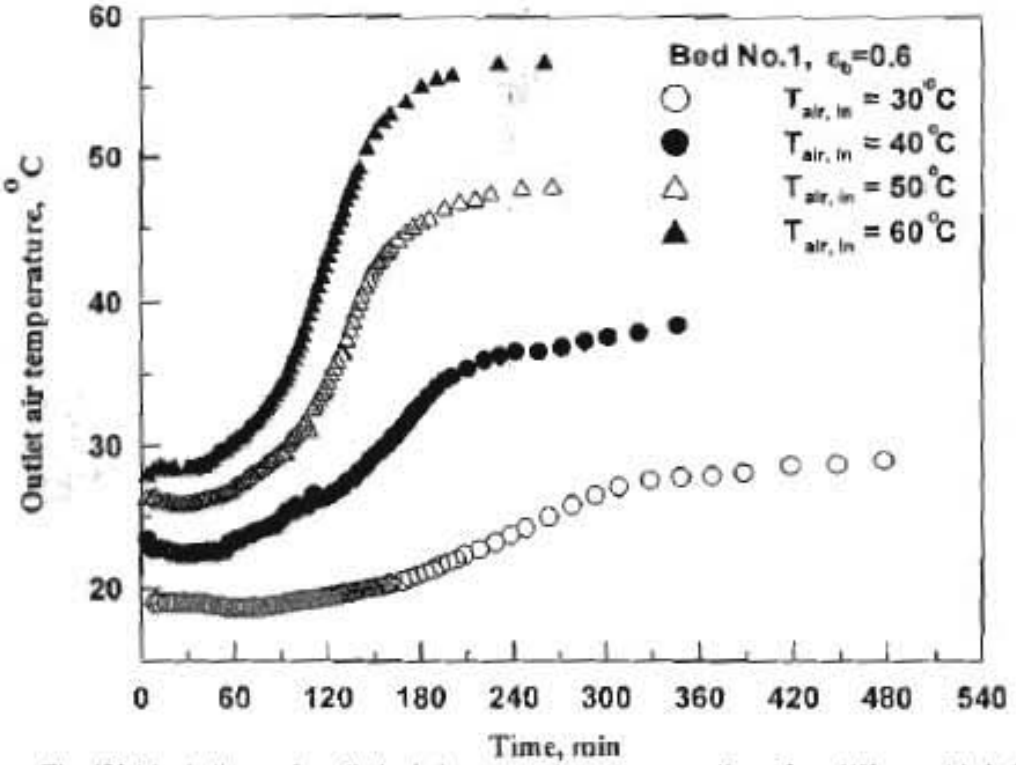

Fig.(2) Variation of outlet air temperature versus time for different inlet air temperatures.

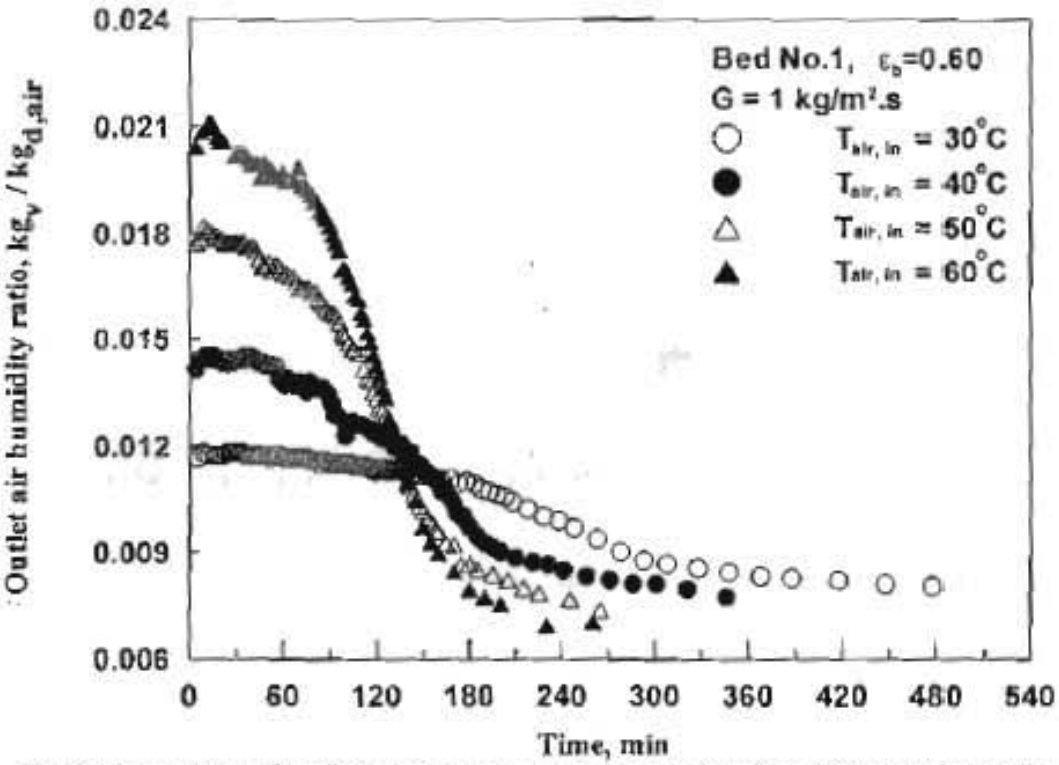

Fig.(3) Variation of outlet air temperature versus time for different inlet air temperatures.

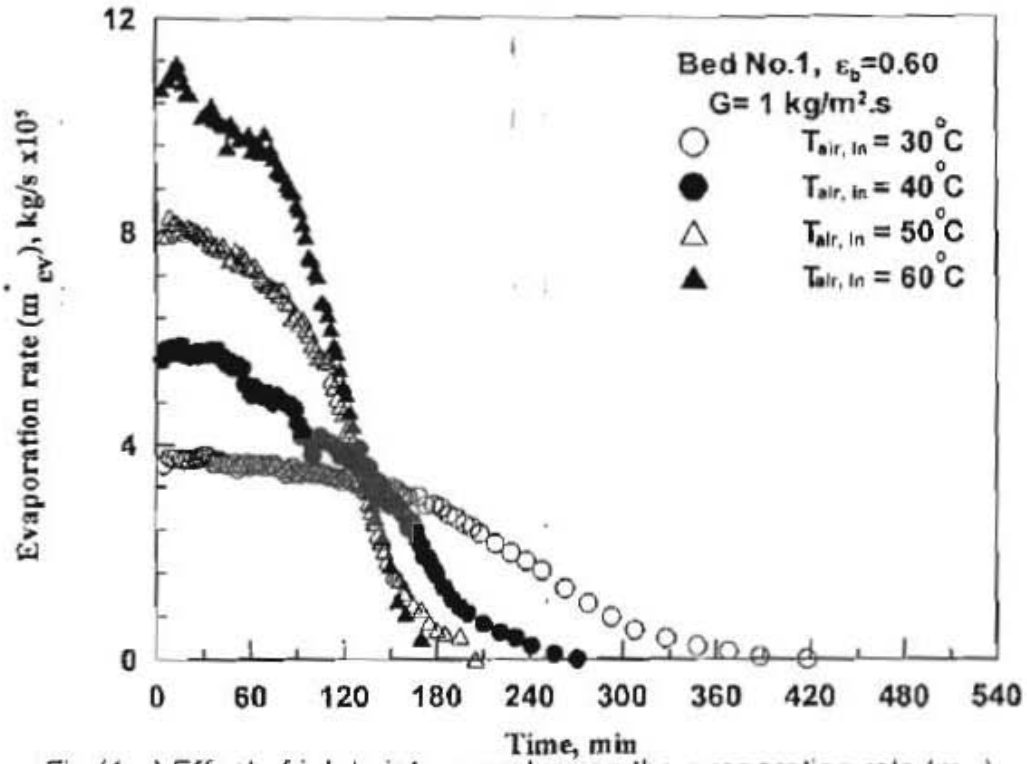

Fig.(4-a) Effect of inlet air temperature on the evaporation rate (m_{ev}).

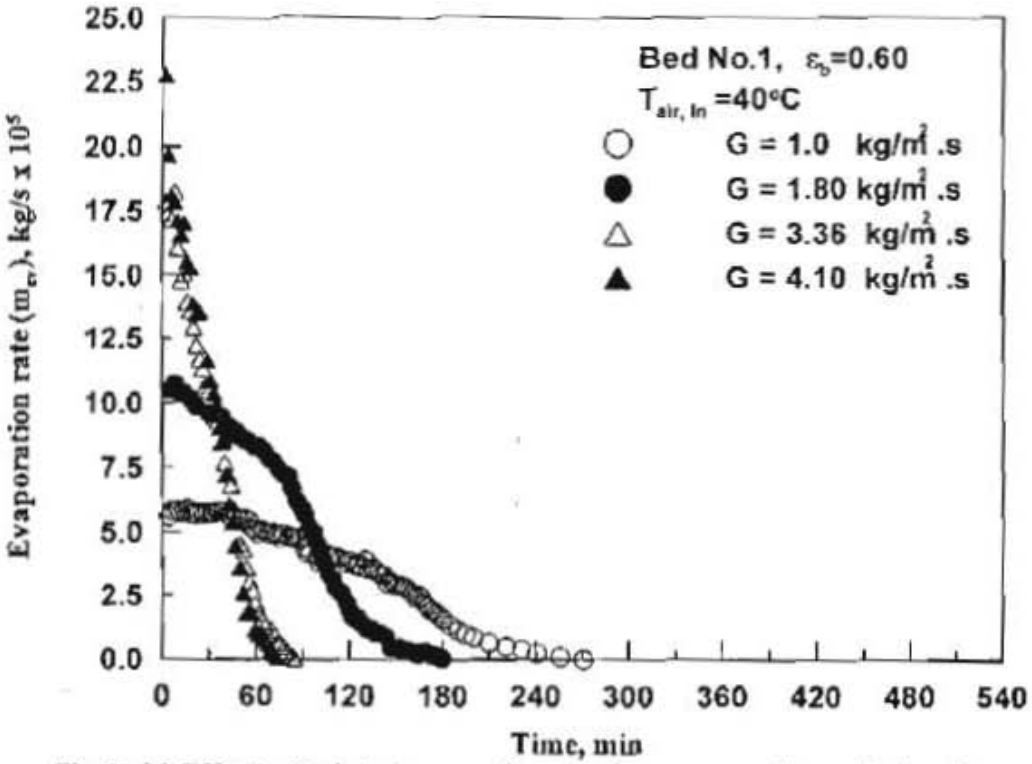

Fig.(4-b) Effect of inlet air mass flux on the evaporation rate (m_{ev}).

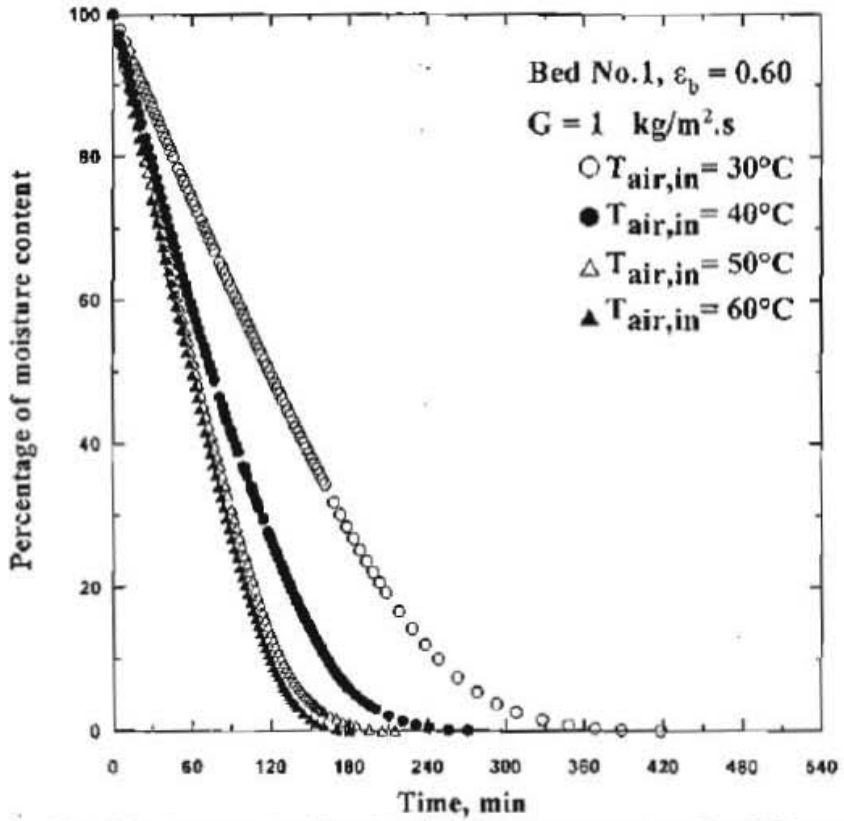

Fig. (5) Percentage of moisture content versus time for different inlet air temperatures.

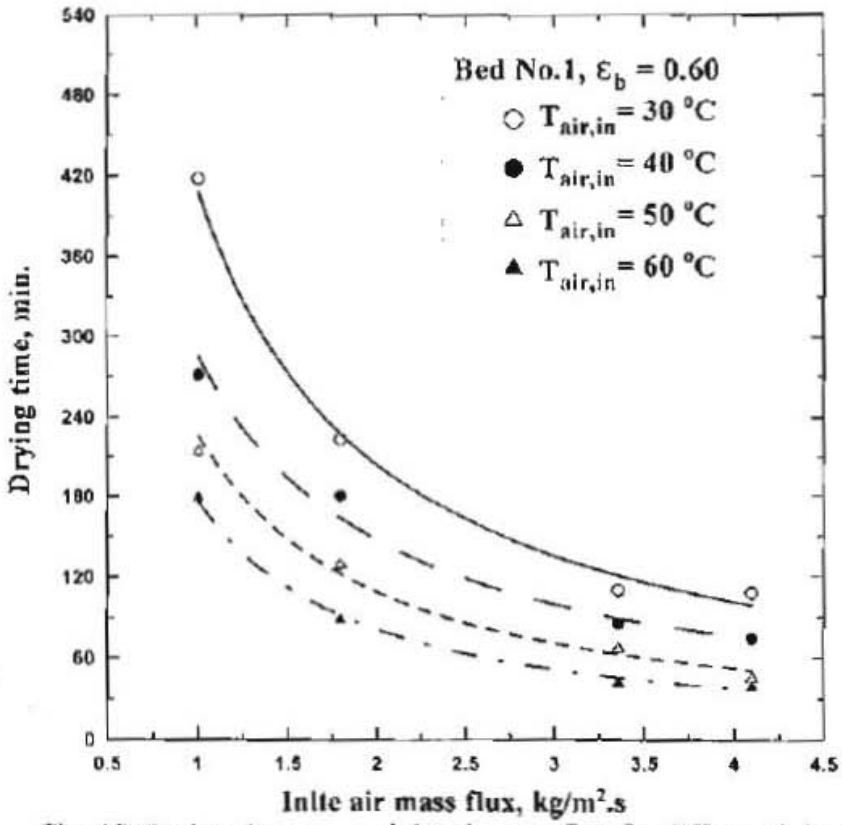

Fig. (6) Drying time versus inlet air mass flux for different inlet air temperatures.

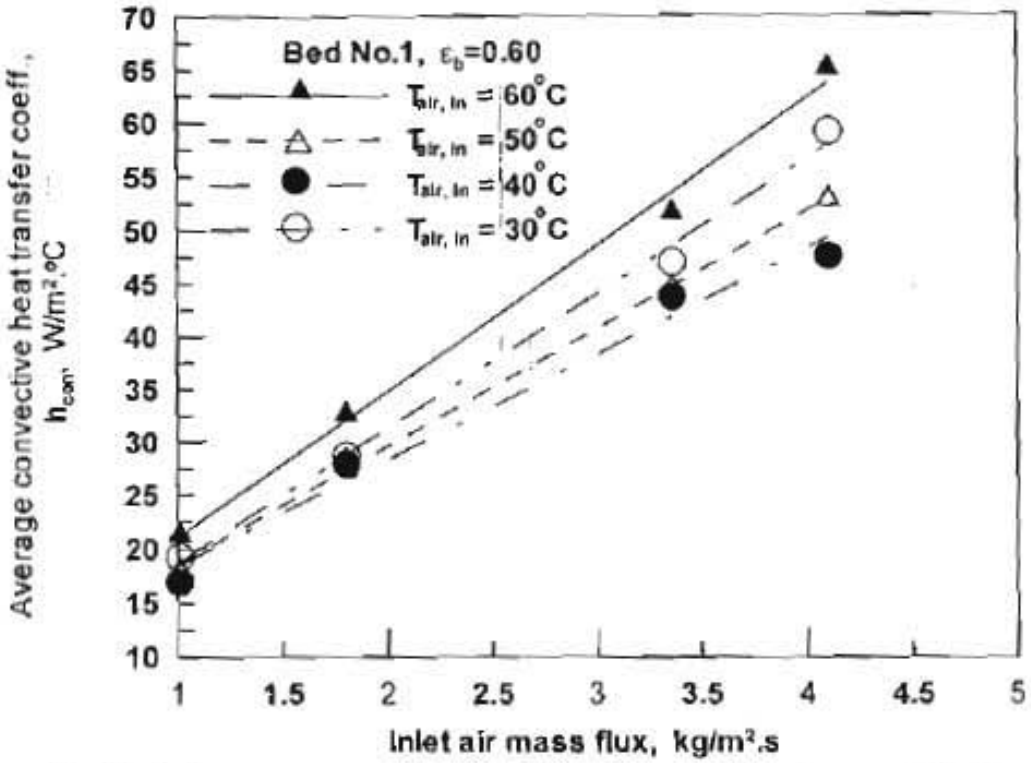

Fig.(7-a) Average convective heat transfer coefficient versus inlet air mass flux for different inlet air temperatures.

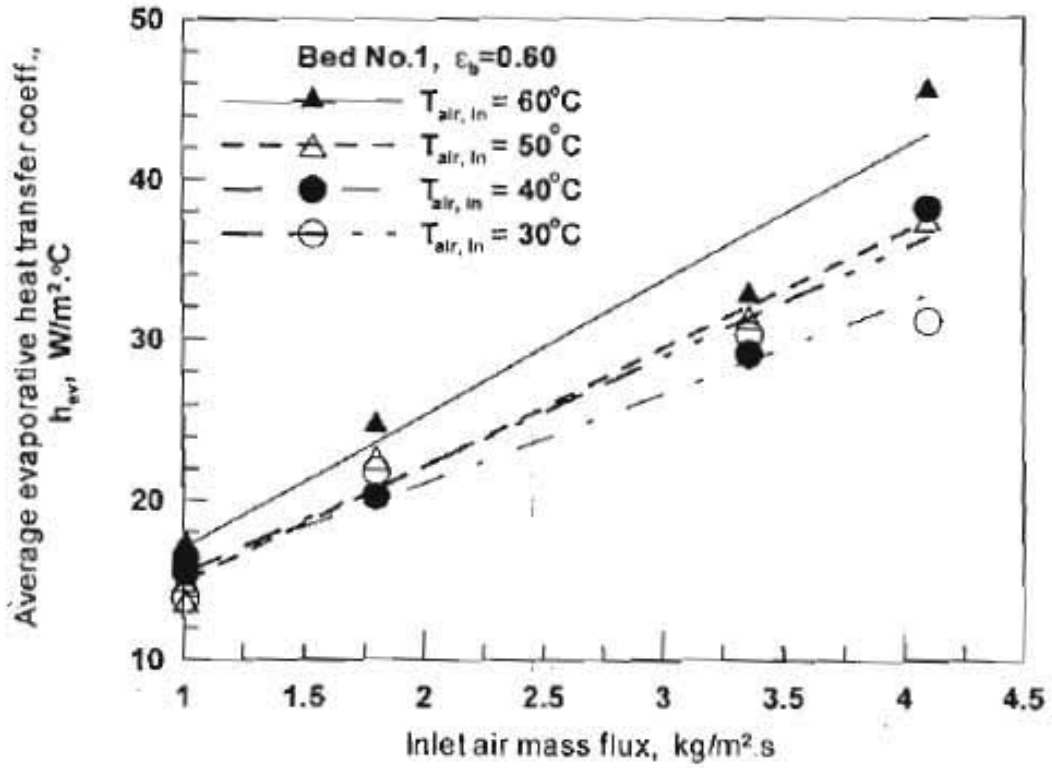

Fig.(7-b) Average evaporative heat transfer coefficient versus inlet air mass flux for different values of inlet air temperatures.

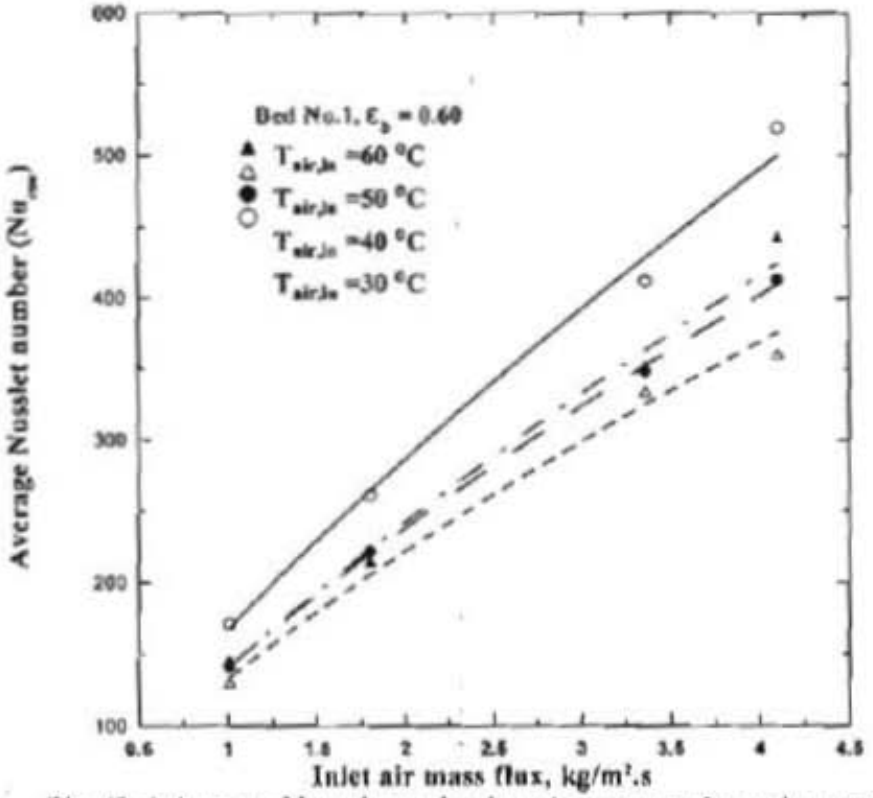

Fig. (8.a) Average Nusselt number based on convection only versus inlet air mass flux for different inlet air temperature.

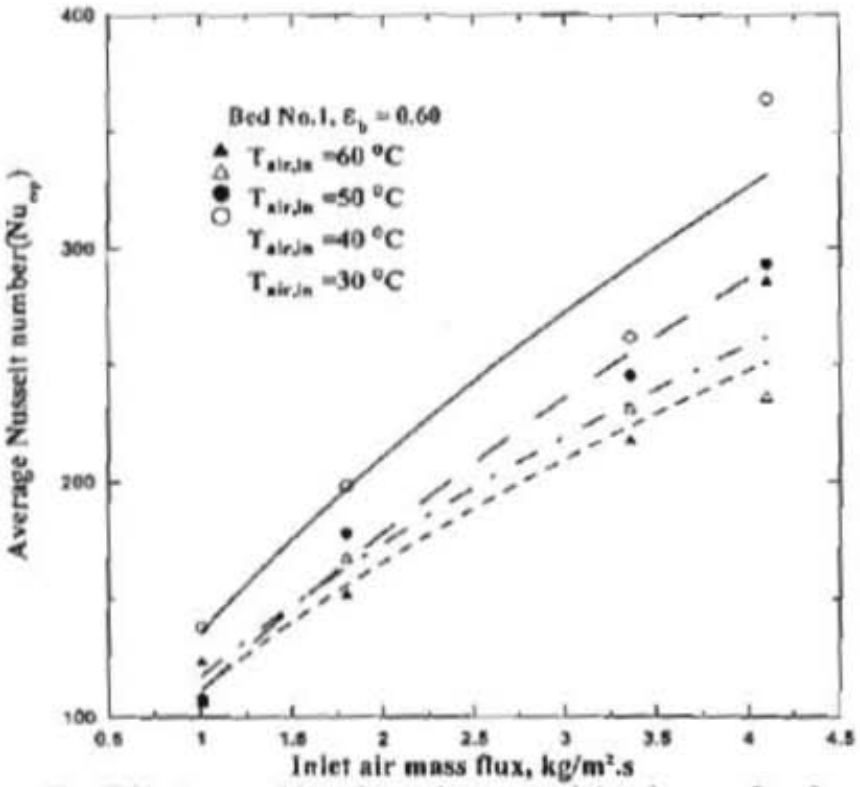

Fig. (8.b) Average Nusselt number versus inlet air mass flux for different inlet air temperature.

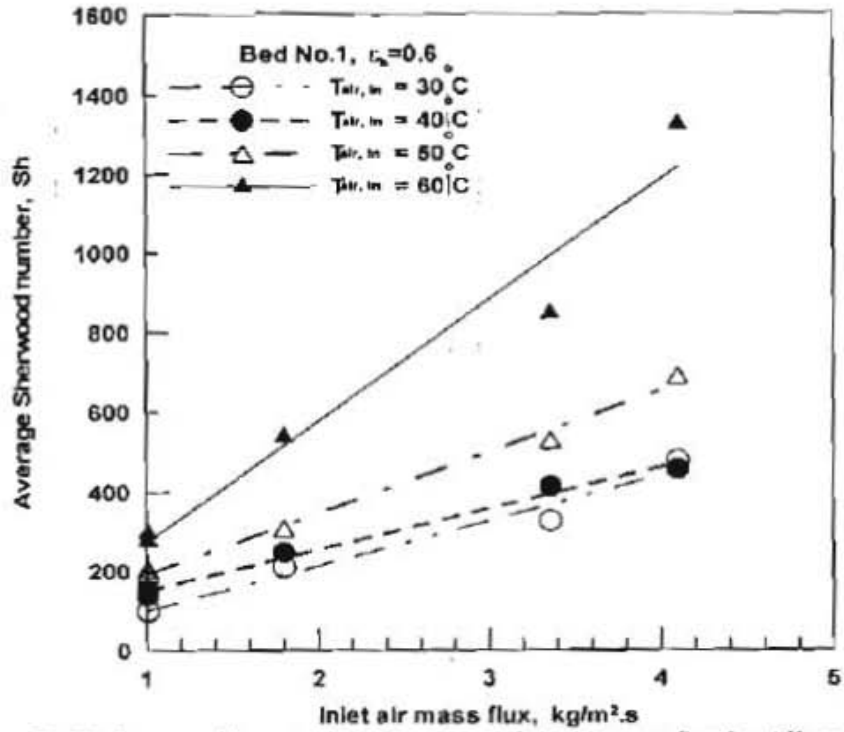

Fig.(9) Average Sherwood number versus inlet air mass flux for different values of inlet air temperatures.

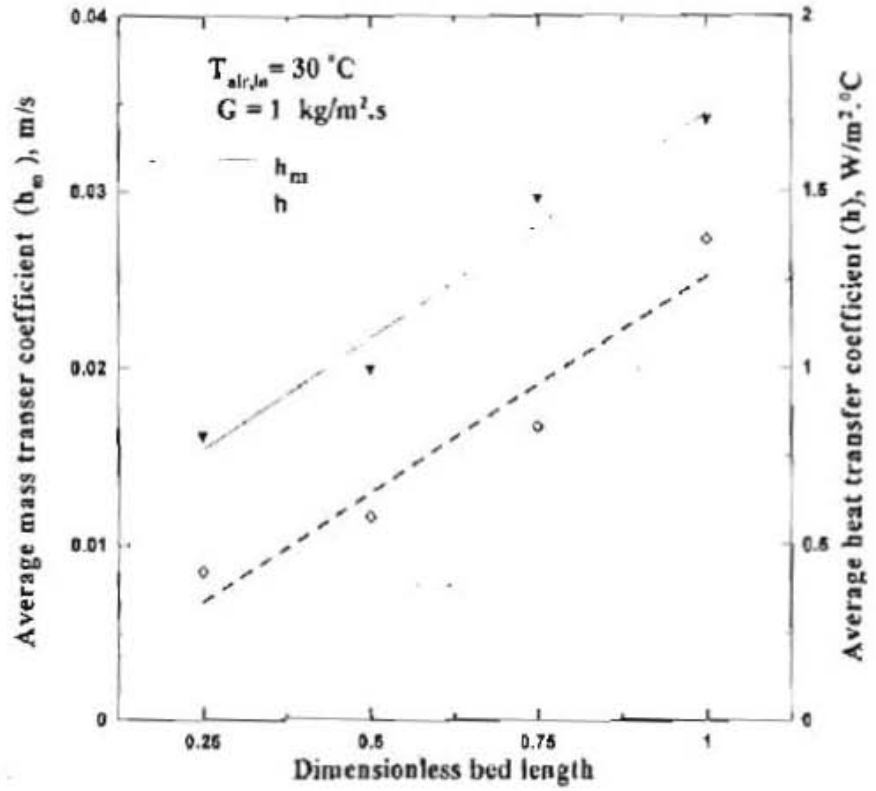

Fig. (10) Effect of dimensionless bed length on the average heat and mass transfer coefficients.

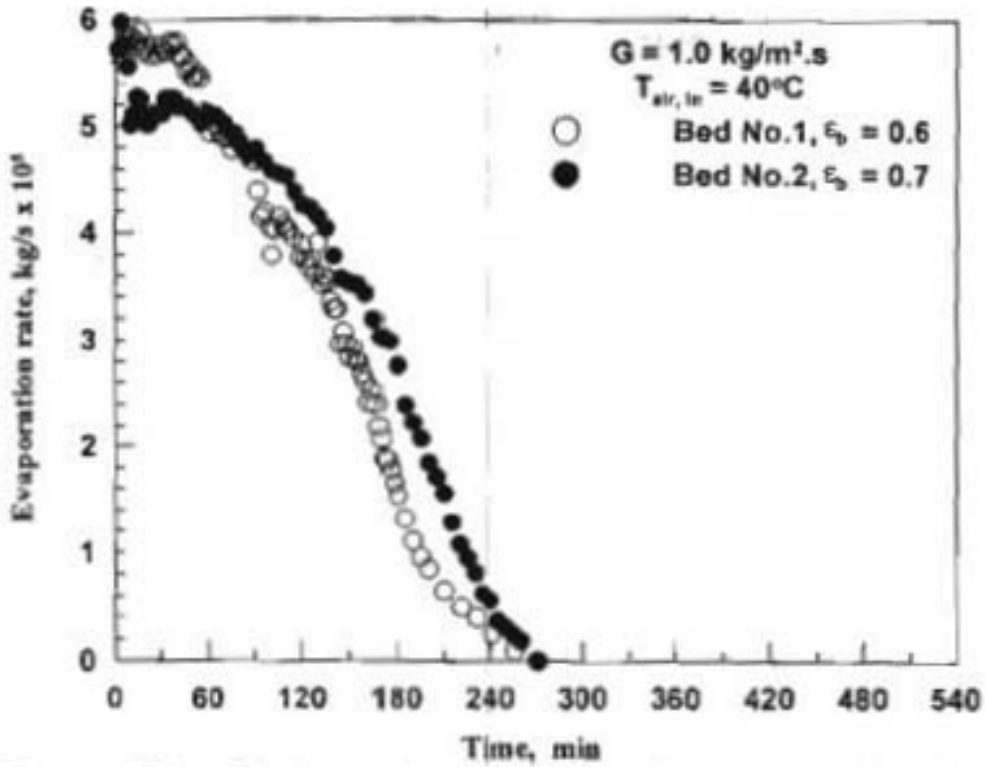

Fig.(11) Effect of ball porosity on the evaporation rate at constant air inlet temperature.

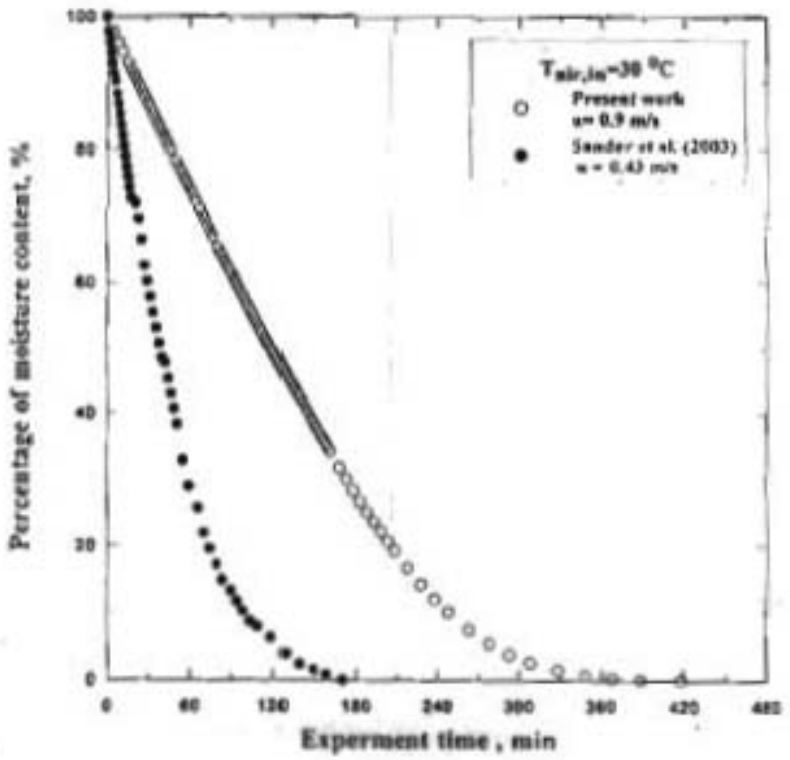

Fig. (12) Comparison of the present experimental results with the previous experimental work.